Ab initio study of thallium nanoclusters on Si(111)-7×7

Geunsik Lee,* Choon Gyu Hwang, Nam Dong Kim, Jinwook Chung, and Jai Sam Kim
Department of Physics, Pohang University of Science and Technology, Pohang, Gyungbuk 790-784, Republic of Korea

Sik Lee
Supercomputing Center, Korea Institute of Science and Technology Information, Daejeon 305-806, Republic of Korea
(Received 23 November 2006; revised manuscript received 24 July 2007; published 10 December 2007)

We have studied the stability of a thallium nanocluster of various numbers of atoms ($N=1,2,\ldots,10$) on a Si(111)-7×7 substrate using density functional theory total energy calculations. We have compared it with clusters of other group III elements (Al, Ga, and In). Thallium is found to be unstable with the triangular cluster, which has been known to be stable for other group III elements. Instead, a slightly different structure, in which Si atop atoms are lower than thallium atoms in height by 2.56 Å, was found to be quite stable. Such an abnormal structure originates from the inert pair of $6s^2$ electrons due to the significant spin-orbit interaction. The initial relaxed $N=6$ Tl cluster continues to grow with increasing N up to $N=9$ in the faulted-half unit cell, which is consistent with experimental observations.

DOI: 10.1103/PhysRevB.76.245409 PACS number(s): 68.43.Bc, 68.43.Hn, 71.15.Mb

I. INTRODUCTION

Self-assembled nanoclusters have attracted much research interest due to their potential applications in microelectronics, ultrahigh-density recording, and nanocatalysis.[1–3] Two of the most commonly used methods, to achieve them, are self-organization in strained homoepitaxial thin-film growth[1,2] and self-assembly in chemical synthesis.[3] The former method yields uniformly sized clusters as well as good spatial distribution. Recently, enhanced-stability clusters on a 7×7 reconstructed Si(111) surface were formed experimentally for various adsorbates, including simple metal[4–7] (Al, Ga, In, and Tl), alkali metal[8] (Na), noble metal[9–11] (Cu, Ag, and Au), transition metal[12] (Co), and group IV elements[13,14] (Sn and Pb). The Si(111)-7×7 surface is a good candidate for surface magic cluster (SMC) creation due to the large potential energy barrier across the half unit cell.

Among the group III elements of SMC on Si(111)-7×7, Tl behaves very differently. For example, two preliminary experimental studies show that Tl behaves either like a monovalent[15] or a trivalent[16] atom. The contradiction was resolved by the report that Tl adsorbate displays a variable valency according to the substrate temperature $T_s \sim 300\ ^\circ\mathrm{C}$ (monovalent below T_s and trivalent above T_s) at a coverage of about 0.3 monolayers.[17] It is believed that such a characteristic is due to the inert pair of $6s^2$ electrons. In the case of Tl SMC on Si(111)-7×7, individual adatoms could not be resolved in the scanning tunneling microscopy (STM) image, which seemingly reflects the high mobility of the Tl adatoms within the cluster.[7] Vitali *et al.*[7] proposed that each Tl cluster consists of nine atoms, which is confirmed also by other measurement.[18] However, SMCs of other group III elements, which are almost the same in shape, show clear atomic spots in STM images. A theoretical model of the cluster, triangular shaped and consisting of six metal adatoms, has been proposed.[19]

In spite of the abnormal properties of Tl, there are very few studies on Tl SMC on Si(111)-7×7. Although there are several theoretical studies on Al, Ga, and In SMCs,[4–6] there has been no theoretical report on any Tl SMC, to the best of our knowledge. In this paper, we report the total energy calculation results for Tl SMCs of various numbers of adatoms on Si(111)-7×7 using the first-principles electronic structure calculation method. We compared the results with those of other group III elements. The calculation methods are described in Sec. II. Our results for the adsorption energies of the Al, Ga, In, and Tl clusters, including a discussion, as well as the electronic band structures of the clean substrate surface and of the Tl SMCs on it, are presented in Sec. III. Finally, conclusions are drawn in Sec. IV.

II. CALCULATION METHODS

The calculations were based on density functional theory[20] and the *ab initio* pseudopotential plane-wave method. The results reported here were obtained with the VASP[21] using the Perdew-Wang 1991 version of the generalized gradient approximation.[22] We used, from the Vienna database,[23] the scalar-relativistic ultrasoft pseudopotential, which provides the recommended energy cutoff for each element. The default plane-wave cutoff of 177 eV, which leads to an error of less than 0.01 eV/atom, was adopted. In the calculation of the electronic density of states and band structures, the spin-orbit interaction was taken into account in the case of the thallium clusters.

We used the slab model of the Si(111)-7×7 dimer-adatom-stacking-fault structure. The slab consists of 6 Si layers, 12 Si adatoms, and 49 H atoms to saturate dangling bonds at the bottom surface. For a six-layer slab, we have 42 surface-layer atoms, 48 second-layer atoms, and 49 atoms for each of the remaining four layers. The unit cell has a total of 298 Si atoms and 49 H atoms. The vacuum region of 10 Å was used. Only the Γ point was used for k-point sampling inside the first Brillouin zone. The Fermi-level smearing approach of Methfessel and Paxton[24] was employed for the electronic states near the Fermi level, with a Gaussian width of 0.2 eV. One bottom layer and H atoms were fixed when relaxing the clean 7×7 surface. Three bottom layers and H

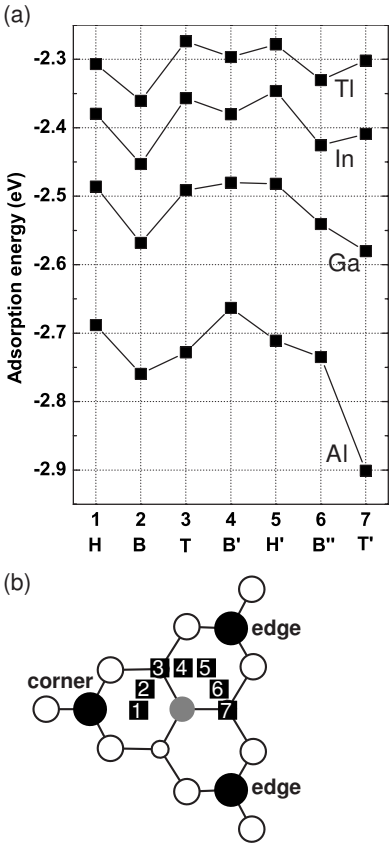

FIG. 1. (a) The energy of a single group III metal atom (Al, Ga, In, and Tl) adsorption at the attractive basin of Si(111)-7×7. (b) Symmetric adsorption sites around the rest atom belonging to the faulted-half unit cell. The adsorption sites indicated by the black rectangles are numbered 1–7 from left to right, clockwise. There are three kinds of adsorption sites, which are top (3,7), bridge (2,4,6), and hollow (1,5) sites. The Si adatom and the Si rest atom are represented by the black and gray circles, respectively. The open circles indicate other Si atoms.

atoms were fixed when relaxing the thallium absorbed surface. Optimized atomic geometries were achieved when the forces on all of the unconstrained atoms were smaller in magnitude than 0.05 eV/Å. These parameters provided for convergence of the total energy to within 0.01 eV/adatom.

III. RESULTS AND DISCUSSIONS

A. Energy of a single atom adsorption

The adsorption energy E_a of a single adsorbate atom is defined as follows:

$$E_a = E_{slab} - E_{clean} - E_{atom}, \quad (1)$$

where E_{slab}, E_{clean}, and E_{atom} are the total energy of the adsorbed surface, the clean surface, and the isolated adsorbate atom, respectively. We calculated the E_{atom} for the spin-polarized configuration. Figure 1 shows the adsorption energies of the metal atoms at each attractive basin[25] of a faulted-half unit cell. There are seven inequivalent high-coordination sites around the rest atom. They are classified into top, hollow, and bridge adsorption sites. Table I lists the sites of the lower adsorption energy for each kind of site, as well as the nearest-neighbor bond lengths of the adsorbate. The lowest-energy sites are the top site (site 7) for Al and Ga and the bridge site (site 2) for In and Tl. The highest-energy sites are the bridge site (4) for Al and Ga, the hollow site (5) for In, and the top site (3) for Tl. On the well-known $\sqrt{3}\times\sqrt{3}$ reconstructed surface, adsorption at the fourfold top site (T4) is 0.30, 0.38, and 0.20 eV/adatom more stable than at the threefold hollow site (H3) for Al, Ga, and In.[26] For Tl, T4 is 0.1 eV/adatom more stable than H3 in the 1×1 phase.[16] However, on the 7×7 reconstructed surface, the bridge site is most stable for In and Tl. The differences between the lowest and highest energies are 0.19, 0.09, 0.07, and 0.06 eV for Al, Ga, In, and Tl, respectively.

Generally, there are two factors governing adatom stability: (i) dangling-bond saturation and (ii) number of bonds. As can be seen in Fig. 1(b), the top site atom saturates one dangling bond of the rest atom, and both the hollow and bridge sites saturate two dangling bonds at the adatom and the rest atom. From Table I, the top site atom has three bonds with Si atoms besides one dangling-bond saturation. The hollow and bridge site atoms have two bonds besides a two dangling-bond saturation, where the bridge site has a shorter bond length than the hollow site. From Fig. 1(a) and Table I, we conclude that factor (ii) is more important for Al and Ga, but that factor (i) becomes more dominant than factor (ii) with increased atomic radius, allowing valence electrons to interact more tightly with dangling bonds.

Interestingly, the outer hollow and bridge sites (sites 1 and 2 in Fig. 1) bonding with a corner Si adatom are more stable than the inner sites (sites 4, 5, and 6) due to the electronic band effect described below. There are a total of 19 dangling-bond electrons coming from 1 corner, 6 rest atoms, and 12 adatoms. Fourteen electrons fill seven surface states, induced by one corner hole and six rest atoms. The remaining five electrons (19−14=5) will occupy the surface states near the Fermi level, induced by Si adatoms. The surface states caused by corner adatoms appear at a lower-energy level than the states induced by the edge adatoms (this will be shown in Sec. III D). Accordingly, the outer-site adsorption, close to the corner adatom, is more stable than the inner site.

We calculated the adsorption energies of a reconstructed surface. According to Ref. 27, the Al adatom on the adatom site of Si(111)-7×7 is more stable than the Si adatom at the same site. Furthermore, the configuration with the Al adatom at the edge site is more stable than the one at the corner site. We considered a configuration in which a metal atom is placed at the edge adatom site, displacing the Si adatom. As for the location of that displaced Si adatom, the total energy calculation with a Si atom adsorbed on the clean Si(111)-7×7 surface showed that the bridge site at the attractive basin is the most stable.[28] We found that the corner bridge site [site 2 in Fig. 1(b)] is the most stable among the three bridge sites for the displaced Si atom. The resulting configuration is shown in Fig. 2. The adsorption energies of the configuration are −3.09, −2.46, −2.06, and −1.59 eV for Al, Ga, In, and Tl, respectively. Compared with the lowest (boldfaced) energies in Table I, only Al has a lower energy, by 0.19 eV, for this configuration, the others have higher energies.

TABLE I. The sites of lower adsorption energy for each of the top, bridge, and hollow sites (see Fig. 1). For each configuration, the nearest-neighbor bond lengths of adsorbate and adsorption energy are given. The bold number indicates the lowest adsorption energy among the three kinds for each adsorbate.

Adsorbate	Site	Bonding distance (Å)[a]	Adsorption energy (eV)[b]
Al	7(T′)	R(2.63), S2(2.58), S1(2.68), S1(2.68)	**−2.90**
	2(B)	Ad(2.68), R(2.84), S1(2.81), S2(3.24)	−2.76
	5(H′)	Ad(2.57), R(2.69), S1(3.03), S1(3.29)	−2.71
Ga	7(T′)	R(2.73), S2(2.73), S1(2.92), S1(2.92)	**−2.58**
	2(B)	Ad(2.74), R(2.90), S1(2.88), S2(3.31)	−2.57
	5(H′)	Ad(2.64), R(2.73), S1(3.09), S1(3.34)	−2.48
In	7(T′)	R(2.94), S2(3.01), S1(3.19), S1(3.19)	−2.41
	2(B)	Ad(2.96), R(3.05), S1(3.09), S2(3.47)	**−2.45**
	1(H)	Ad(2.92), R(2.92), S1(3.63), S1(3.63)	−2.38
Tl	7(T′)	R(2.98), S2(3.12), S1(3.34), S1(3.34)	−2.30
	2(B)	Ad(3.05), R(3.09), S1(3.30), S2(3.63)	**−2.36**
	1(H)	Ad(2.97), R(3.08), S1(3.78), S1(3.78)	−2.31

[a]Ad: nearby adatom, R: rest atom, S1: first-layer atom except the rest atom, S2: second-layer atom.
[b]The definition is given by Eq. (1).

We also calculated the adsorption energies in the unfaulted-half unit cell at the lowest-energy site. This site is equivalent to the most stable position of the faulted-half unit cell. The adsorption energies are −2.89, −2.57, −2.40, and −2.30 eV for Al, Ga, In, and Tl. The lowest-energy site in the unfaulted-half unit cell yields 0.01, 0.01, 0.05, and 0.06 eV higher energies than the site in the faulted-half unit cell for each adsorbate.

B. Magic clusters of Al, Ga, and In

A few years ago, magic clusters of Al, Ga, and In on Si(111)-7×7 were formed by subtle variation of the deposition condition. As the theoretical structural model of the cluster, the triangular shape shown in Fig. 3 was proposed.[19] The cluster consists of six metal atoms, where three atoms each are located at the corner and at the edge. The three edge Si adatoms, which we will call atop Si atoms, are displaced toward the center. The metal atoms at the edge are higher than those at the corner and lower than the atop Si atoms. Our calculated atomic structures of Al, Ga, and In clusters are in reasonable agreement with the results of Ref. 19. The atop Si atoms are 0.78, 0.66, and 0.55 Å higher than the corner metal atoms for Al, Ga, and In, respectively.

We calculated the adsorption energies of the clusters shown in Fig. 3. The adsorption energy $E_a(N)$ is given by

$$E_a(N) = [E_{slab}(N) - E_{clean}]/N - E_{atom}, \tag{2}$$

where $E_{slab}(N)$, E_{clean}, and E_{atom} are the total energy of the N adsorbates adsorbed surface, the clean surface, and the iso-

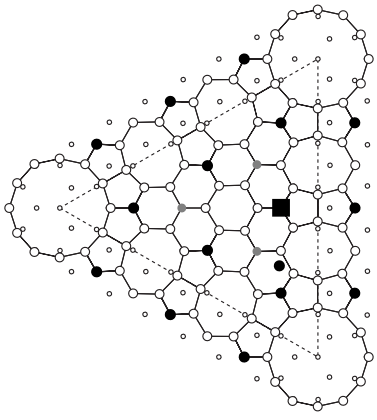

FIG. 2. Top view of a single metal atom adsorption on the faulted-half unit cell of Si(111)-7×7, where the metal atom is placed at the edge adatom site, displacing the Si adatom. The displaced Si adatom is most stable at the corner bridge site (see the text). The black, gray, and open circles represent the Si adatom, the rest atom, and the other Si atoms, respectively. The metal atom is indicated by a black rectangle.

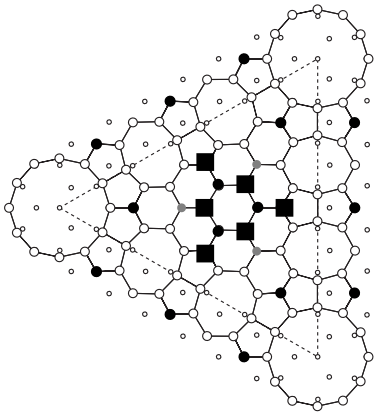

FIG. 3. Top view of the triangular cluster of Al, Ga, and In on the faulted-half unit cell of Si(111)-7×7. The cluster consists of six metal atoms. The symbols have the same meanings as in Fig. 2.

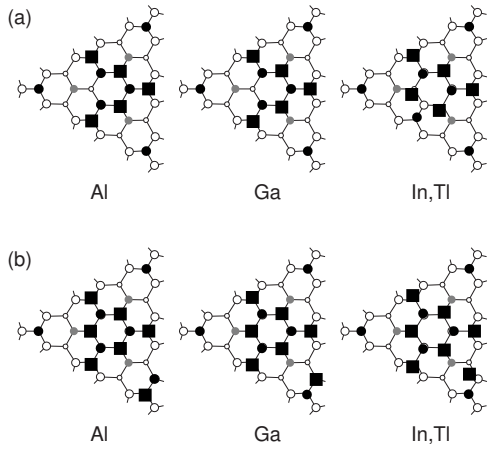

FIG. 4. Top views of the most stable clusters of Al, Ga, In, and Tl for (a) $N=5$ and (b) $N=7$ (see the text). The symbols have the same meanings as in Fig. 2.

lated adsorbate atom. The values of $E_a(N=6)$ are −3.93, −3.24, and −2.78 eV/adatom for Al, Ga, and In. The energies are 1.03, 0.66, and 0.33 eV lower than the lowest energies of a single atom adsorption (Table I) for Al, Ga, and In, respectively. This indicates the high stability of the cluster. In order to confirm the magic $N=6$ cluster, we calculated the adsorption energies for the most stable $N=5$ and 7 clusters.

For $N=5$, there are two possibilities in detaching a metal atom from the $N=6$ cluster. We can take out a corner or an edge metal atom. For Al and Ga, the removal of the edge metal atom yields a 0.10 and a 0.04 eV/adatom lower adsorption energy than the removal of the corner atom, respectively. However, the corner metal atom removal yields a lower energy for In, where the difference is 0.04 eV/adatom. For the most stable clusters with $N=5$, as shown in Fig. 4(a), the values of $E_a(N=5)$ are −3.69, −3.03, and −2.64 for the clusters of Al, Ga, and In, respectively. We also calculated the energy of the sixth atom adsorption in the $N=5$ cluster, which is defined as $E_{slab}(N=6)-E_{slab}(N=5)-E_{atom}$. They are −5.10, −4.27, and −3.45 eV for the clusters of Al, Ga, and In. The energies are 2.20, 1.69, and 1.00 eV lower than the lowest adsorption energies of the clean surface (Table I). This confirms the enhanced stability of the $N=6$ cluster.

For $N=7$, we recollect that the most stable top site is already occupied by the edge metal atom. It is desirable, then, for a metal atom to be placed at the outer bridge site [site 2 in Fig. 1(b)] because this site has the next lowest energy, as shown in Fig. 1 and Table I. The other point is that a metal atom can yield a lower energy when it is placed at the corner adatom site, displacing the corner Si adatom. The displaced Si atom is initially placed at the nearby bridge site and is relaxed during the calculation. Hence, we calculated the total energies of the $N=7$ clusters with the seventh metal atom placed at the bridge site or the corner adatom site. For Al, the placement at the corner adatom site, displacing the Si adatom to the top of the Si atom on the surface layer, yields a 0.01 eV/adatom lower energy than placement at the bridge site. For Ga, the seventh metal atom initially at the bridge site is relaxed to the top of the Si atom on the surface layer. The energy is 0.05 eV/adatom lower than the energy of the metal atom at the corner adatom site. For In, the metal atom at the bridge site yields a 0.10 eV/adatom lower energy than the one at the corner adatom site. The most stable clusters with $N=7$ are shown in Fig. 4(b). The values of $E_a(N=7)$ are −3.74, −3.12, and −2.69 for the clusters of Al, Ga, and In, respectively. We calculated the adsorption energies, defined as $E_{slab}(N=7)-E_{slab}(N=6)-E_{atom}$, from the $N=6$ to $N=7$ clusters. They are −2.62, −2.41, and −2.18 eV for the clusters of Al, Ga, and In. These energies are 0.28, 0.17, and 0.27 eV higher than the lowest adsorption energies on the faulted half of the clean surface (Table I) for Al, Ga, and In. They are also higher than the adsorption energies on the unfaulted half of the clean surface. Therefore, it is likely that the metal atoms form a triangular cluster until both half units of the clean surface are filled with the clusters. This results in homogeneous clusters with a good spatial distribution.

The important energy values in our calculations are summarized in Table II, together with Tl. Group III elements, except for thallium, form enhanced-stability triangular clusters at $N=6$. Thereby, we can confirm the magic geometry in submonolayer growth of group III metal atoms on Si(111)−7×7, except for thallium.

C. Tl cluster

As shown in Table II, a thallium cluster of the triangular shape is not stable. In order to find a stable cluster of Tl, we calculated the adsorption energy [Eq. (2)] with respect to the number of thallium atoms N.

TABLE II. Important adsorption energy values (in eV) for Al, Ga, In, and Tl clusters (the value in parentheses is the difference relative to the $N=1$ case). The second row ($N=1$; recon) is the adsorption energy of the reconstructed surface, in which a metal atom is adsorbed at the edge adatom site, displacing the edge Si adatom (see Fig. 2). The configurations for $N=5,7$ and $N=6$ are shown in Figs. 4 and 3, respectively.

	Al	Ga	In	Tl
$N=1$	−2.90	−2.58	−2.45	−2.36
$N=1$; recon	−3.09	−2.46	−2.06	−1.59
δE $(N=1,\mathrm{UH})^a$	0.01	0.01	0.05	0.06
$(N=5)\rightarrow(N=6)$	−5.10(−2.20)	−4.27(−1.69)	−3.45(−1.00)	−1.94(0.42)
$(N=6)\rightarrow(N=7)$	−2.62(0.28)	−2.41(0.17)	−2.18(0.27)	−2.40(−0.04)

[a]The difference in energies of a metal atom adsorption onto the unfaulted half (UH) and the faulted half (FH): the FH is more stable than the UF.

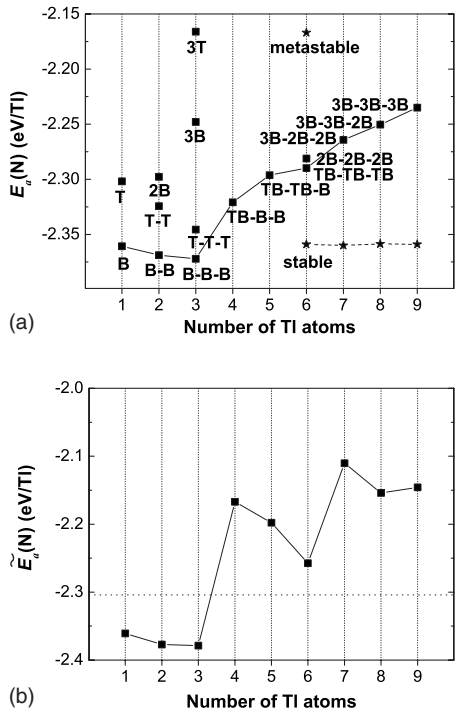

FIG. 5. (a) The adsorption energies of the thallium cluster given by Eq. (2) for $1 \leqslant N \leqslant 9$, where N is the number of Tl atoms of the cluster. See the text for the meaning of the configuration symbols. The rectangle and star symbols represent the cases of no reconstruction and reconstruction of the substrate, respectively (see the text). The lowest-energy configurations are joined together by a solid line (a dashed line), the atomic structures of which are shown in Fig. 6 (Fig. 7). (b) The energies of the last Tl atom adsorption, defined by Eq. (3), of the lowest E_a configurations in (a) for the case of no reconstruction (Fig. 6).

In finding the lowest-energy cluster for each N, first, we considered the case in which the Si(111)-7×7 surface structure remains unchanged by the Tl atom adsorption (we call this "no reconstruction"). The favorable sites for adsorption are determined by the adatom-substrate and adatom-adatom interactions. The adatom-substrate interaction is illustrated in Fig. 1. The adatom-adatom interaction was examined by varying the distance among adatoms, each of which is placed in the basins of the faulted-half unit cell.

The results are shown in Fig. 5(a) and are indicated by the rectangles. The symbol of each cluster is described below. The clean surface has three attractive basins per half unit cell. Each basin has stable adsorption sites: bridge (B), top (T), and hollow (H). The number before the site symbol denotes the number of the same kind of adsorption sites. Different basins are partitioned by a hyphen (-). For example, 3B has three Tl atoms at the bridge sites in one basin. B-B-B has one atom at the bridge site per basin.

For each N, we considered several seemingly low-energy configurations. Some of them are displayed in the figure for $1 \leqslant N \leqslant 9$. Top views of the lowest-energy clusters are shown in Fig. 6. Thallium is very different from the other group III elements in that the triangular $N=6$ cluster [indicated by "metastable" in Fig. 5(a)] lacks the minimal energy. Instead,

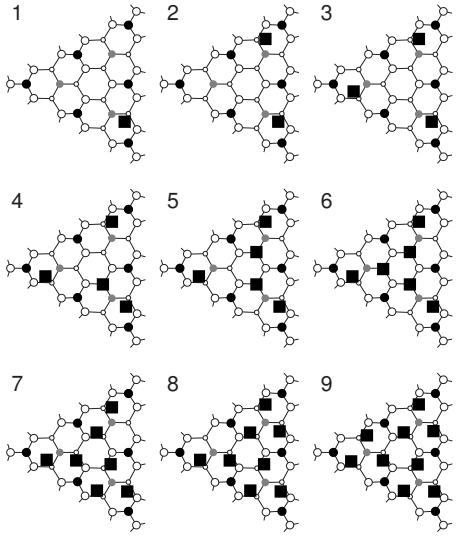

FIG. 6. Top views of the Tl clusters on the faulted-half unit cell of Si(111)-7×7 with the lowest energy for each N. They correspond to the case of no reconstruction (see the text). The symbols have the same meanings as in Fig. 2.

the $N=3$ cluster has the minimal energy in the case of no reconstruction, as shown in Fig. 5(a).

The lowest-energy site for $N=1$ is the outer bridge site (site 2 in Fig. 1). To see the variation of $E_a(N)$ to $N=3$, we tried the two methods for placing the second and third atoms. They are (i) all adatoms inside one basin and (ii) one adatom per basin. In case (i), the energy increases with N, as shown by B, 2B, and 3B in Fig. 5(a). We see the same trend at the top site (T, 3T). The reason for the increase is that the second and third adatoms cannot gain energy from dangling-bond saturation of the Si rest atom. However, the energy decreases slightly in case (ii). In particular, the top site (T is the inner top site, as indicated by site 7 in Fig. 1) yields a much larger decrease. The interaction between the Tl adatoms results in such a decrease of energy. Due to the shorter Tl-Tl distance for the inner top sites than that for the bridge sites, T-T-T should experience a much larger decrease of energy than B-B-B.

From the B-B-B cluster, we found that the top site is stable for an additional adsorption of one ($N=4$) or two ($N=5$) Tl atoms. For $N=6$, we placed one Tl atom per basin at the bridge site for T-T-T or B-B-B. Then, we obtained the configurations of two Tl atoms at the top and bridge sites (TB-TB-TB) or at the bridge sites (2B-2B-2B), per basin. The energy of TB-TB-TB is 9 meV/Tl lower than that of 2B-2B-2B. Going from $N=6$ to $N=9$, we placed Tl atoms at the bridge site. The final $N=9$ cluster consists of three Tl atoms within each basin at the bridge sites.

Our adsorption energy results obtained without reconstruction do not agree with the experimental result of Ref. 7, which proposed that the number of atoms per Tl cluster created in the faulted half should be close to nine with the $N=9$ structural model shown in Fig. 6. In order to find the largest number of atoms per cluster that can be formed in the faulted half without adsorption onto the unfaulted half, we calculated the differential adsorption energy,[29] which is defined as follows:

$$\tilde{E}_a(N) = E_{slab}(N) - E_{slab}(N-1) - E_{atom}, \quad (3)$$

for the lowest-energy configurations illustrated in Fig. 5(a). The magnitude of $\tilde{E}_a(N)$ gives the energy gain per Tl atom if an additional Tl atom is adsorbed at a surface which is already covered with $(N-1)$ Tl atoms. By definition, $\tilde{E}_a(N=1)$ is the same as $E_a(N=1)$ of Eq. (2). If $\tilde{E}_a(N)$ for an additional Tl adsorption onto the faulted half is higher than the adsorption energy onto the unfaulted half, Nth Tl atom will be adsorbed onto the unfaulted half. Here, $\tilde{E}_a(N)$ are shown in Fig. 5(b) together with the lowest energy of adsorption in the unfaulted region for the clean surface (indicated by a dotted horizontal line). Up to $N=3$, the Tl atoms will be adsorbed in the faulted half because the energy is about 0.06 eV/Tl lower than the horizontal line. For $N \geqslant 4$, however, the energy is higher than the lowest energy of adsorption onto the unfaulted half, which is not consistent with the experiment in the case of no reconstruction.

We then tried to find a low-energy cluster by reconstructing the Si(111)-7×7 surface structure. As a starting geometry, we considered the triangular $N=6$ cluster, shown in Fig. 3, where the adsorption energy is marked by a star with the annotation metastable in Fig. 5(a) [$E_a(N=6)$ is -2.17 eV/Tl]. The three Si atop atoms are higher than the other metal atoms in Fig. 3, but we made the edge Tl atoms to be the highest, the corner atoms to be the next highest, and the Si atop atoms to be the lowest in the cluster. After the relaxation of that initial geometry, the resulting $E_a(N=6)$ is -2.36 eV/Tl which is 0.19 eV/Tl lower than the energy of the metastable cluster. The energy is indicated by the star with the annotation "stable" in Fig. 5(a). Based on the obtained stable $N=6$ cluster, we calculated the energies of the $N=7$ cluster in which the seventh Tl atom is placed on the top, bridge, and hollow sites in the basin. The top site was found to be the most stable. The bridge and hollow sites had 0.02 and 0.03 eV/Tl higher energies than that of the top, respectively. By placing one Tl atom at the top site of each basin, we obtained the stable $N=9$ cluster, as shown in Fig. 7.

The lowest-energy site for the seventh Tl adsorption was calculated to be the top site ("2" in Fig. 7) rather than the bridge site for a single atom adsorption as in Fig. 1. Since two or three Tl atoms inside one basin lead to a higher energy than one Tl atom due to the less dangling-bond saturation at the rest atom, all the seventh adsorption sites are expected to give higher energies than the lowest $E_a(N=1)$ at the bridge site. However, the top site is significantly stabilized by the bonding with neighboring Tl adatom ("4" in Fig. 7), where the bond length (3.38 Å) is comparable to the bulk Tl-Tl bond length (3.40 Å). The resulting $E_a(N=7)$ is eventually the same as the lowest $E_a(N=1)=-2.36$ eV/Tl. The eighth or ninth adsorption onto other basins should give almost the same energies due to the weak interbasin interactions.

Thallium adatoms in the stable $N=9$ cluster have different heights with respect to the corner Si adatom in the faulted-half unit cell, as indicated in Fig. 7. The highest Tl atom (4) is 2.06 Å higher than the Si adatom. Taking into account the atomic radii of Tl and Si (1.7 and 1.2 Å), the relative height of the highest Tl, when probing the electron density, was found to be 2.56 Å. This is perfectly consistent with the result by the STM experiment, which reported a height difference of about 2.5 Å.[7]

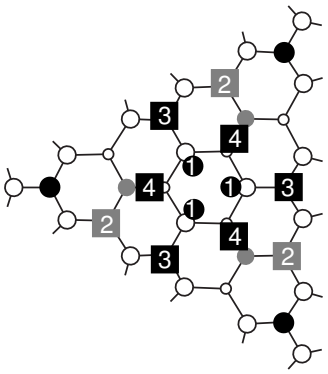

FIG. 7. Top view of the $N=9$ Tl cluster on the faulted-half unit cell of Si(111)-7×7 with the lowest energy for the case of reconstruction. The heights relative to the corner Si adatom are 0.93, 1.10, 1.21, and 2.06 Å for the adatoms marked by 1, 2, 3, and 4, respectively. The $N=9$ cluster is obtained by placing three Tl atoms at the outer top sites (indicated by gray rectangles and 2) in the stable $N=6$ cluster. The symbols have the same meanings as in Fig. 2.

We need to account for why the energy of the stable $N=6$ cluster is much lower than that of the metastable cluster. That phenomenon is caused by the inert pair effect of Tl $6s^2$. The effect originates from the spin-orbit interaction, where a larger energy is required to promote s electrons to form sp hybridization in a heavier element such as thallium. In the metastable cluster, thallium atoms have bond lengths of 2.7–2.8 Å along Si atoms with the coordination of three, where the bond length among Si atops is 4.2 Å. In the stable cluster, the bonds among Si atops become stronger with bond lengths of 2.5 Å; thus, the bonds between thallium atoms and Si atoms are weakened with bond lengths of 3.0–3.3 Å. As a result, the thallium valence shell electrons contributing to the bond are fewer in the stable cluster. Actually, the numbers of s electrons inside a sphere of radius 1.7 Å are 0.84 and 0.47 per thallium atom for the stable and the metastable clusters, respectively. This means that the stable cluster hybridizes the s orbital of thallium to a lesser extent with p orbital, which is favored by the thallium atom. Therefore, the stable cluster has a lower energy than the metastable cluster.

In order to find the maximal number of atoms in each cluster without adsorption onto the unfaulted half, we calculated the energies of an additional Tl atom adsorption onto the unfaulted half for the "reconstruction" cluster of $N=6$, 7, 8, or 9 on the faulted half. Then, we compared them with the adsorption energies for the stable clusters of $N=7$, 8, 9, and 10. The results are presented in Table III. Up to $N=9$, the adsorption onto the faulted half results in lower energy (by 0.02–0.03 eV/Tl) than that onto the unfaulted half. Therefore, Tl atoms favor the formation of clusters in the faulted half up to $N=9$. At $N=10$, however, the unfaulted half is 0.03 eV/Tl more stable than the faulted half. Thus, we can confirm that Tl clusters will be formed in the faulted half

TABLE III. The energies of the $(N+1)$th thallium atom adsorption onto the FH and the UH unit cell in the stable reconstruction cluster with N thallium atoms. The adsorption sites for FH and UF are the top and bridge sites, respectively.

N before adsorption	$(N+1)$th on FH	$(N+1)$th on UF
6	−2.37	−2.34
7	−2.35	−2.33
8	−2.36	−2.33
9	−2.29	−2.32

with nine atoms per cluster, as reported in Ref. 7.

The obtained $N=9$ cluster has a quite low energy, where E_a $(N=9)$ is 0.124 eV/Tl lower than that of no-reconstruction cluster for $N=9$ from Fig. 5(a). Although the proposed model for $N=9$ cluster is not reconstructed like 3B-3B-3B in Fig. 5(a), it is not exactly the cluster observed in the experiment.[7] Among the possible atomic configurations that we have attempted, the cluster of Fig. 7 appears to be the most stable atomic structure for a $N=9$ Tl nanocluster formed in the faulted half.

In the experimental STM image, the atomic spots were not resolved but blurred due to the high mobility of the Tl adatoms within the clusters.[7] To unravel such question, we calculated the energy barrier of the Tl atoms rotating around the remaining atoms for the two $N=9$ clusters, which are 3B-3B-3B in Fig. 5(a), and for the stable cluster, shown in Fig. 7. In the 3B-3B-3B cluster, three Tl atoms inside one basin are rotated through the top site or the hollow site, while the six other Tl atoms in other basins are kept fixed. The energy barriers were determined to be 0.07 and 0.10 eV/Tl through the top and hollow sites, respectively. In the stable cluster, one Tl atom, indicated by 2 in Fig. 7, is moved through the outer bridge and hollow sites. The energy barrier was 0.23 eV/Tl. Since the energy barriers for Tl diffusion are found to be much greater than thermal energy at room temperature (RT), Tl diffusion at RT should not be the sole reason for the blurred STM images.

All of the results obtained in this calculation assume zero temperature. In order to find the atomic structure of a cluster observed at RT, the effect of finite temperature should be considered, as should the reaction path and energy. It is still possible that the atomic structure of a cluster at RT may be slightly modified from the one we suggest in Fig. 7 due to temperature effect. Experimentally, several phases were detected by STM above RT (~300 °C),[30] which indicates the prevalent effect of the temperature. Therefore, more studies should be undertaken in order to find the atomic structure of the RT cluster.

D. Electronic structures

Figure 8 shows the projected electronic density of states (DOS) and band structure for the clean surface. There are three well-known surface states; S_1, S_2, and S_3. Of the 19 dangling-bond electrons in the 7×7 surface, 14 fill seven dangling-bond states induced by one corner hole and six rest

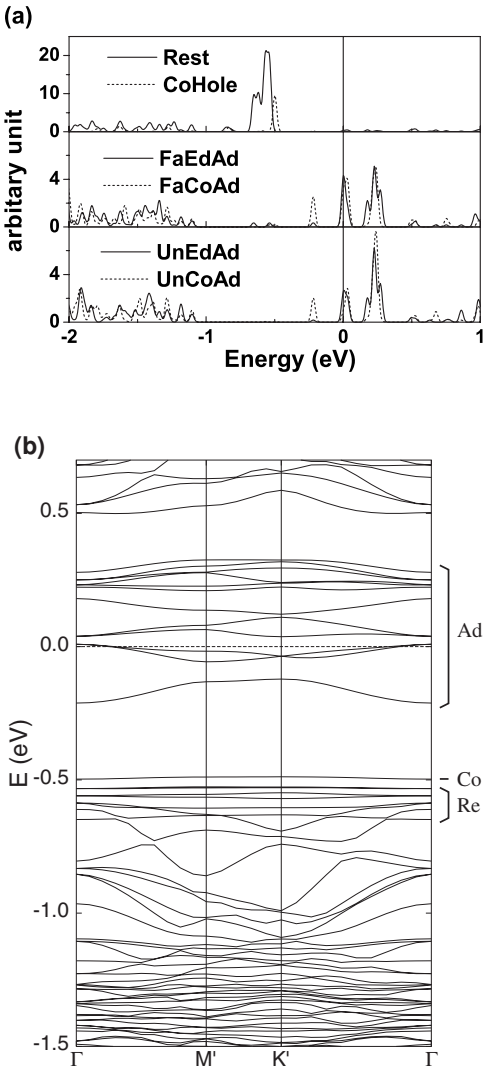

FIG. 8. (a) Projected electronic density of states for the clean Si(111)-7×7 surface. Rest, CoHole, and {Fa,Un}{Ed,Co}Ad mean six rest atoms, one corner hole, and three {faulted,unfaulted} {edge,corner} adatoms. (b) Band structure of the clean surface. The origins of the surface states are indicated on the right side of the plot. Ad, Co, and Re mean adatoms, corner hole, and rest atoms, respectively.

atoms. The remaining five electrons should fill two and half surface states caused by 12 adatoms near the Fermi level. We can see such features from the projected DOS shown in Fig. 8(a). The S_3 states below −1.0 eV mainly come from the Si adatoms, which are very broad in energy. The S_2 states near −0.6 eV are caused by the rest atoms. They overlap with the corner-hole-induced surface state. The S_1 states, which are induced by the Si adatoms, have three peaks at −0.2, 0.0, and 0.2 eV. The number of states belonging to each peak is one, four, and seven, respectively. Interestingly, the first peak of the S_1 states is mostly caused by the corner Si adatoms. This result suggests that adsorption sites corresponding to the corner adatom dangling-bond saturation should have lower energy than those corresponding to the edge adatom, which is already shown in Fig. 1. Also, the faulted region has a slightly larger electron population than the unfaulted one (1.3

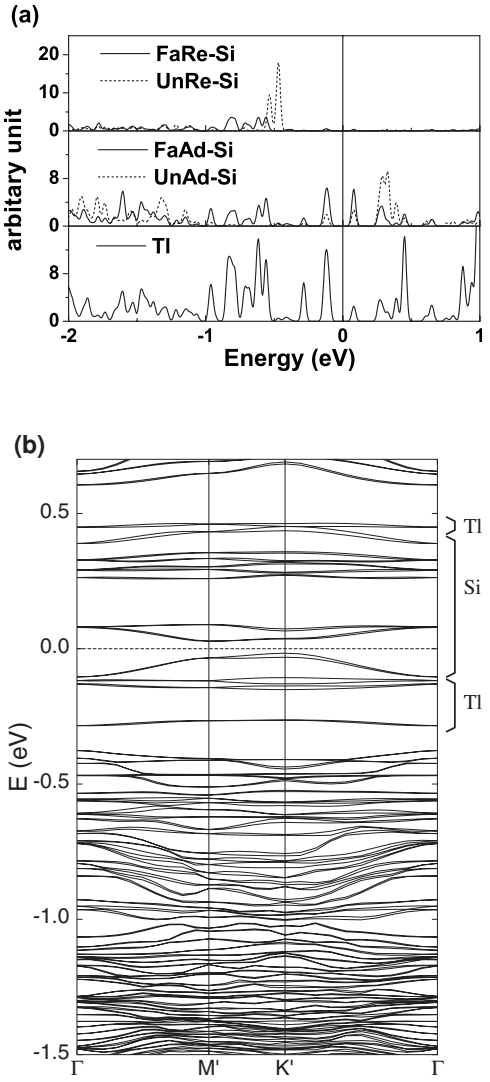

FIG. 9. (a) Projected electronic density of states for the thallium $N=9$ cluster (see Fig. 7) adsorbed on Si(111)-7×7. {Fa,Un}{Re,Ad}-Si and Tl mean {faulted,unfaulted} Si {rest atoms, adatoms} and nine Tl adatoms, respectively. (b) Band structure. Tl and Si on the right side mean that the surface states are induced by thallium and silicon atoms, respectively.

times larger for the first peak). This means that the faulted half is more preferable to the unfaulted half in filling the adatom dangling-bond states and lowering the total energy. Thus, the symmetric site on the faulted half has a slightly lower energy than the equivalent on the unfaulted half, which is shown in Table II. In Fig. 8(b), the band structure is shown together with the surface states S_1 (Ad: adatoms) and S_2 (Co: corner hole; Re: rest atoms).

Figure 9 shows the projected DOS and band structure for the stable thallium $N=9$ cluster adsorbed on Si(111)-7×7, where the spin-orbit interaction was taken into account. The thallium adsorbate causes the S_2 and S_1 surface states concerned with the rest and the Si adatoms on the faulted half to move left (to lower energies) due to the bonding between the Si atoms and the Tl adatoms. Upon the adsorption of the thallium atoms, the system becomes a semiconductor for which the energy gaps are 0.18, 0.06, and 0.05 eV at each k point of Γ, M′ and K′, respectively, as shown in Fig. 9(b). As can be seen in the band structure, 2 of the 18 Si-adatom-induced states are filled. This can be explained by the fact that three Si adatoms participate in the bonding in a thallium cluster; thus, there remain a total of 16 dangling-bond electrons instead of 19 for the clean surface. Of the 16 dangling-bond electron, 14 fill 12 surface states induced by 6 rest atoms and 2 states by the corner hole atom (note the spin up and spin down states for each dangling-bond state). The remaining two electrons will occupy two Si adatom states, as shown in the band structure.

IV. SUMMARY

We have investigated energetics of atomic clusters of several atomic species (Al, Ga, In, and Tl) formed on the Si(111)-7×7 surface. The change of adsorption energy E_a as a function of number of constituent atoms (N) in a single cluster on a frozen substrate exhibits a minimum at $N=6$ for Al, Ga, and In clusters in agreement with previous calculations and recent STM observations.

The behavior of $E_a(N)$ on the frozen substrate, however, appears to be quite different for Tl cluster, showing a minimum at $N=3$ and then gradual increase with N. By relaxing the substrate Si atoms (reconstructed), we find that $E_a(N)$ reaches a minimum at $N=9$ with 0.124 eV/Tl lower than that of the frozen cluster. All Tl adatoms occupy high symmetry sites only in faulted-half unit cell up to $N=9$, while the tenth Tl adatom favors a site in unfaulted-half unit cell. We thus determined the stable atomic arrangement of a single Tl cluster composed of nine Tl atoms with three central Tl atoms bulging over the corner Si adatoms by 2.56 Å, which is in excellent accord with 2.5 Å determined in STM study. Since the energy barrier between high symmetry sites (0.23 eV) appears to be much greater than thermal energy at room temperature, the blurred STM images of Tl clusters apparently demand an explanation based on atomic structure fully taking into account of temperature effect. The unique features of Tl clusters distinct from other atomic clusters consisting of six atoms are ascribed mainly to the inert pair of $6s^2$ electrons due to the significant spin-orbit interaction.

ACKNOWLEDGMENTS

We would like to thank Byung Deok Yu for the helpful discussions. This work was supported by Postech BSRI Research Fund 2006. We would like to acknowledge the support from KISTI (Korea Institute of Science and Technology Information) under The Strategic Supercomputing Support Program. J.C. acknowledges support from the Korea Research Foundation Grants (KRF-2006-312-C00513).

*maxgeun@physics.postech.ac.kr

[1] K. Bromann, C. Félix, H. Brune, W. Harbich, R. Monot, J. Buttet, and K. Kern, Science **274**, 956 (1996).
[2] H. Brune, M. Glovannini, K. Bromann, and K. Kern, Nature (London) **394**, 451 (1998).
[3] S. Sun, C. B. Murray, D. Weller, L. Folks, and A. Moser, Science **287**, 1989 (2000).
[4] J. Jia, J.-Z. Wang, X. Liu, Q.-K. Xue, Z.-Q. Li, Y. Kawazoe, and S. B. Zhang, Appl. Phys. Lett. **80**, 3186 (2002); V. G. Kotlyar, A. V. Zotov, A. A. Saranin, T. V. Kasyanova, M. A. Cherevik, I. V. Pisarenko, and V. G. Lifshits, Phys. Rev. B **66**, 165401 (2002).
[5] M. Y. Lai and Y. L. Wang, Phys. Rev. B **64**, 241404(R) (2001); H. H. Chang, M. Y. Lai, J. H. Wei, C. M. Wei, and Y. L. Wang, Phys. Rev. Lett. **92**, 066103 (2004).
[6] J.-L. Li, J.-F. Jia, X.-J. Liang, X. Liu, J.-Z. Wang, Q.-K. Xue, Z.-Q. Li, J. S. Tse, Z. Zhang, and S. B. Zhang, Phys. Rev. Lett. **88**, 066101 (2002).
[7] L. Vitali, M. G. Ramsey, and F. P. Netzer, Phys. Rev. Lett. **83**, 316 (1999).
[8] K. Wu, Y. Fujikawa, T. Nagao, Y. Hasegawa, K. S. Nakayama, Q. K. Xue, E. G. Wang, T. Briere, V. Kumar, Y. Kawazoe, S. B. Zhang, and T. Sakurai, Phys. Rev. Lett. **91**, 126101 (2003).
[9] Y. P. Zhang, L. Yang, Y. H. Lai, G. Q. Xu, and X. S. Wang, Surf. Sci. **531**, L378 (2003).
[10] T. Jarolímek, J. Mysliveček, P. Sobotík, and I. Oŝt'ádal, Surf. Sci. **482-485**, 386 (2001); P. Sobotík, I. Oŝt'ádal, and P. Kocán, *ibid.* **507-510**, 389 (2002); I. Oŝt'ádal, P. Kocán, P. Sobotík, and J. Pudl, Phys. Rev. Lett. **95**, 146101 (2005).
[11] S. K. Ghose, P. A. Bennett, and I. K. Robinson, Phys. Rev. B **71**, 073407 (2005).
[12] M. A. K. Zilani, Y. Y. Sun, H. Xu, Y. P. Feng, X.-S. Wang, and A. T. S. Wee, Phys. Rev. B **72**, 193402 (2005).
[13] O. Custance, I. Brihuega, J. M. Gómez-Rodríguez, and A. M. Baró, Surf. Sci. **482-485**, 1406 (2001).
[14] S.-C. Li, J.-F. Jia, R.-F. Dou, Q.-K. Xue, I. G. Batyrev, and S. B. Zhang, Phys. Rev. Lett. **93**, 116103 (2004).
[15] C. Castellarin-Cudia, S. Surnev, M. G. Ramsey, and F. P. Netzer, Surf. Sci. **491**, 29 (2001).
[16] S. S. Lee, H. J. Song, K. D. Kim, J. W. Chung, K. Kong, D. Ahn, H. Yi, B. D. Yu, and H. Tochihara, Phys. Rev. B **66**, 233312 (2002).
[17] V. G. Kotlyar, A. A. Saranin, A. V. Zotov, and T. V. Kasyanova, Surf. Sci. **543**, L663 (2003).
[18] N. D. Kim, C. G. Hwang, Y. Kim, T. C. Kim, D. Y. Noh, K. Sumitani, H. Tajiri, O. Sakata, and J. W. Chung, Surf. Sci. (to be published).
[19] J.-F. Jia, X. Liu, J.-Z. Wang, J.-L. Li, X. S. Wang, Q.-K. Xue, Z.-Q. Li, Z. Zhang, and S. B. Zhang, Phys. Rev. B **66**, 165412 (2002).
[20] P. Hohenberg and W. Kohn, Phys. Rev. **136**, B864 (1964); W. Kohn and L. J. Sham, Phys. Rev. **140**, A1133 (1965).
[21] G. Kresse and J. Hafner, Phys. Rev. B **47**, 558 (1993); G. Kresse and J. Furthmüller, *ibid.* **54**, 11169 (1996).
[22] J. P. Perdew and Y. Wang, Phys. Rev. B **45**, 13244 (1992).
[23] D. Vanderbilt, Phys. Rev. B **41**, 7892 (1990); G. Kresse and J. Hafner, J. Phys.: Condens. Matter **6**, 8245 (1994).
[24] M. Methfessel and A. T. Paxton, Phys. Rev. B **40**, 3616 (1989).
[25] K. Cho and E. Kaxiras, Europhys. Lett. **39**, 287 (1997); K. Cho and E. Kaxiras, Surf. Sci. **396**, L261 (1998).
[26] J. M. Nicholls, B. Reihl, and J. E. Northrup, Phys. Rev. B **35**, 4137 (1987).
[27] H. Uchida, T. Kuroda, F. Mohamad, J. Kim, K. Nishimura, and M. Inoue, Surf. Sci. **566-568**, 197 (2004).
[28] C. M. Chang and C. M. Wei, Phys. Rev. B **67**, 033309 (2003).
[29] S. Wilke, D. Hennig, and R. Lober, Phys. Rev. B **50**, 2548 (1994).
[30] A. V. Zotov, A. A. Saranin, V. G. Kotlyar, O. A. Utas, and Y. L. Wang, Surf. Sci. **600**, 1936 (2006).